Journal of Low Temperature Physics, Vol. 17, Nos. 1/2, 1974

t-Matrix Calculation of the Ground-State Energies of Solid ^{3}He

V. Canuto* and J. Lodenquai*

NORDITA, Copenhagen, Denmark

L. Parish

Department of Physics, University of Florida, Gainesville, Florida

and S. M. Chitre

Tata Institute of Fundamental Research, Bombay, India

(Received March 14, 1974)

The analysis of the Bethe–Goldstone equation for solid ^{3}He is performed by removing the difficulties of symmetry encountered in a previously published version of the problem. Better agreement with experimental data is obtained. The new form of the Bethe–Goldstone two-body equation has special significance for problems related to fission and to solidification of neutron matter.

1. INTRODUCTION

In three previous publications[1–3] (hereafter referred to as I, II, and III respectively), a self-consistent t-matrix method was used to calculate the ground-state energies of solid ^{3}He, solid H_2, and solid neutrons. The two-body wave function ψ_{12} satisfies the simplified Bethe–Goldstone equation, known as the Iwamoto–Namaizawa–Guyer–Zane (INGZ) equation

$$[T_1 + T_2 + U(1) + U(2) + V_{12}]\psi_{12} = E_{12}\psi_{12} \tag{1}$$

where T_1 and T_2 are the kinetic energy operators of particles 1 and 2, respectively; $U(i)$ is the self-consistent one-body potential for the ith particle; and V_{12} is the two-body potential. $U(i)$ was assumed to be a harmonic oscillator potential of the form

$$U(i) = U(0) + \tfrac{1}{2}m\omega^2(\mathbf{r}_i - \mathbf{R}_i)^2 \tag{2}$$

*Permanent Address: Institute for Space Studies, Goddard Space Flight Center, New York.

where m is the mass of the particle, ω the oscillation frequency, $\mathbf{r}_i$ the coordinate of the ith particle at any moment, and $\mathbf{R}_i$ its lattice site. If $V_{12} = 0$, ψ_{12} then reduces to the product of two Gaussians, and E_{12} would be just $2[\frac{3}{2}\hbar\omega + U(0)]$.

In terms of "relative" and "center-of-mass" coordinates $\mathbf{r}$ and $\mathbf{R}$ respectively, (1) reduces to

$$[-(\hbar^2/m)\nabla_r^2 + U(\mathbf{r}) + V(\mathbf{r})]\psi(\mathbf{r}) = (E_{12} - \tfrac{3}{2}\hbar\omega)\psi(\mathbf{r}) \tag{3}$$

where

$$U(1) + U(2) = U(\mathbf{r}) + U(\mathbf{R})$$
$$U(\mathbf{R}) = m\omega^2[\mathbf{R} - \tfrac{1}{2}(\mathbf{R}_1 + \mathbf{R}_2)]^2$$
$$U(\mathbf{r}) = 2U(0) + \tfrac{1}{4}m\omega^2(\mathbf{r} - \Delta)^2, \qquad \Delta = \mathbf{R}_2 - \mathbf{R}_1$$

Equation (3) can be rewritten

$$[-(\hbar^2/m)\nabla_r^2 + \tfrac{1}{4}m\omega^2 r^2 - \tfrac{1}{2}m\omega^2\mathbf{r}\cdot\Delta + V(\mathbf{r})]\psi(\mathbf{r}) = E'_{12}\psi(\mathbf{r}) \tag{4}$$

where

$$E'_{12} \equiv E_{12} - 2U(0) - \tfrac{3}{2}\hbar\omega - \tfrac{1}{4}m\omega^2\Delta^2$$

The INGZ equation was solved numerically by expanding $\psi(\mathbf{r})$ in terms of partial waves, which resulted in a set of coupled differential equations for the various partial waves. The reader should consult I and II for full details.

The presence of the $\mathbf{r}\cdot\Delta$ term in the INGZ equation is undesirable since it couples the lth partial wave state to the $(l \pm 1)$th states. Thus the $\mathbf{r}\cdot\Delta$ term admits states that are not allowed by the Pauli principle. For example, in the neutron solid computation, where $V(\mathbf{r})$ depends on the spin and angular momentum states, the $^1S_0$ state would be coupled to the $^1P_1$ state, which is forbidden by the Pauli principle. In paper II, where the neutron solid was studied, these "unwanted" waves were eliminated by making different approximations. Clearly, these unwanted waves would not enter if $U(\mathbf{r})$ were invariant under space inversion. The main object of this paper is to find a $U(\mathbf{r})$ that is invariant under space inversion and then use it to calculate the ground-state energy of solid ^{3}He. A similar scheme was mentioned by Brandow.[4] The inclusion of this symmetric $U(\mathbf{r})$ in the neutron solid computation should automatically exclude the unwanted waves in the set of coupled equations. The neutron solid computation using the symmetric $U(\mathbf{r})$ derived in this paper is now being carried out.

2. SYMMETRIC $U(\mathbf{r})$

We require the INGZ equation for two particles in the $V_{12} = 0$ case to be

$$[T_1 + T_2 + U_s(1,2)]\phi^{\pm}(1,2) = E_0^{\pm}\phi^{\pm}(1,2) \tag{5}$$

where $\phi^{\pm}(1,2)$ are properly antisymmetrized wave functions for the two particles. These antisymmetrized wave functions require $U_s(1,2)$ to be symmetric under particle exchange. For each particle the equation of motion is simply

$$[T_1 + U(1)]\phi_1(1) = [\tfrac{3}{2}\hbar\omega + U(0)]\phi_1(1) \tag{6}$$

where $U(1)$ is given by Eq. (2) and $\phi_1(1)$ is a Gaussian given by

$$\phi_1(1) \equiv \phi_{R_1}(\mathbf{r}_1) = \frac{\alpha^{3/2}}{\pi^{3/4}} \exp\left[-\frac{\alpha^2}{2}(\mathbf{r}_1 - \mathbf{R}_1)^2\right]; \qquad \alpha^2 = \frac{m\omega}{\hbar} \tag{7}$$

We choose $E_0^{\pm} = 3\hbar\omega + 2U_0$ in Eq. (5). The basis of this choice is that this eigenvalue is the same as that of the unperturbed, unsymmetrized, relative coordinate case. Similarly, $\phi^{\pm}(1,2)$ is chosen to be the properly symmetrized product of Gaussians, i.e.,

$$\phi^{\pm}(1,2) = (1/\sqrt{2})[\phi_1(1)\phi_2(2) \pm \phi_2(1)\phi_1(2)] \tag{8}$$

In terms of $\mathbf{r}$ and $\mathbf{R}$, Eq. (8) reads

$$\phi^{\pm}(1,2) = 2^{-1/2}\Phi(\mathbf{R})[\phi_d(\mathbf{r}) \pm \phi_x(\mathbf{r})] \tag{9}$$

where $\Phi(\mathbf{R})$ is the "center-of-mass" wave function given by

$$\Phi(\mathbf{R}) = \frac{\alpha^{3/2}}{(\pi/2)^{3/4}} \exp\left[-\alpha^2\left(\mathbf{R} - \frac{\mathbf{R}_1 + \mathbf{R}_2}{2}\right)^2\right] \tag{10}$$

and

$$\begin{aligned} \phi_d(\mathbf{r}) &= \frac{\alpha^{3/2}}{(2\pi)^{3/4}} \exp\left[-\frac{\alpha^2}{4}(\mathbf{r} - \Delta)^2\right] \\ \phi_x(\mathbf{r}) &= \frac{\alpha^{3/2}}{(2\pi)^{3/4}} \exp\left[-\frac{\alpha^2}{4}(\mathbf{r} + \Delta)^2\right] \end{aligned} \tag{11}$$

In Eq. (8) the plus (minus) sign corresponds to the spin singlet (triplet) case. In terms of $\mathbf{r}$ and $\mathbf{R}$, Eq. (5) now reduces to

$$\left[-\frac{\hbar^2}{4m}\nabla_R^2 - \frac{\hbar^2}{m}\nabla_r^2 + U_s(1,2)\right]\phi^{\pm}(1,2) = [3\hbar\omega + 2U(0)]\phi^{\pm}(1,2) \tag{12}$$

If we write

$$U_s(1,2) \equiv U_s(\mathbf{R}) + U_s(\mathbf{r}) \tag{13}$$

Eq. (11) becomes

$$[-(\hbar^2/m)\nabla_r^2 + U_s(\mathbf{r}) + \tfrac{3}{2}\hbar\omega]\phi^{\pm}(\mathbf{r}) = [3\hbar\omega + 2U(0)]\phi^{\pm}(\mathbf{r}) \tag{14}$$

where

$$U_s(\mathbf{R}) = m\omega^2[\mathbf{R} - \tfrac{1}{2}(\mathbf{R}_1 + \mathbf{R}_2)]^2 \tag{15}$$

Since

$$\nabla_r^2\phi^{\pm}(\mathbf{r}) = -\frac{\alpha^2}{2\sqrt{2}}\left\{\left[3 - \frac{\alpha^2}{2}(\mathbf{r} - \Delta)^2\right]\phi_d(\mathbf{r}) \pm \left[3 - \frac{\alpha^2}{2}(\mathbf{r} + \Delta)^2\right]\phi_x(\mathbf{r})\right\} \tag{16}$$

we can finally solve for $U_s(\mathbf{r})$, thus obtaining

$$U_s^{\pm}(\mathbf{r}) = 2U(0) + \tfrac{1}{4}m\omega^2\left[r^2 + \Delta^2 - 2\mathbf{r}\cdot\Delta\begin{cases}\tanh(\frac{1}{2}\alpha^2\mathbf{r}\cdot\Delta) & S = 0\\ \operatorname{cotanh}(\frac{1}{2}\alpha^2\mathbf{r}\cdot\Delta) & S = 1\end{cases}\right] \tag{17}$$

We notice that $U_s^{\pm}(\mathbf{r})$ is now symmetric with respect to the transformation $\mathbf{r} \to -\mathbf{r}$. However, when $\frac{1}{2}\alpha\mathbf{r}\cdot\Delta \gg 1$, Eq. (17) reduces in form to the $U(r)$ used in I.

The form of $U_s(r)$ contains a great deal of structure, which is exhibited in Figs. 1 and 2. In Fig. 1 we plot

$$f(r) = r^2 + \Delta^2 - 2\mathbf{r}\cdot\Delta\tanh(\tfrac{1}{2}\alpha^2\mathbf{r}\cdot\Delta) \tag{18}$$

versus r for fixed Δ and ω (or α^2) for different values of θ, the angle between $\mathbf{r}$ and Δ. It is seen that for $\mathbf{r} \perp \Delta$ (an improbable geometric configuration), $f(r) \sim r^2 + \Delta^2$ and the potential has no spikes in the middle. In the most probable configuration, $\theta = 0$, $f(r)$ has a very pronounced central barrier whose height depends on the value of Δ. In order to exhibit the dependence of $U_s(r)$ on various shells of a bcc structure, we plot $f(x)$ versus x at $\theta = 0$ for the first, fifth, and tenth shells in Fig. 2. As expected, the further away the shell, the more pronounced the central barrier, making the tunneling process highly improbable. A high tunneling probability is found, however, for the first shell, whose contribution to the ground-state energy is the most conspicuous. We do not plot $U(S = 1)$ because it is very similar and nothing new would be learned from the graphs, whose main purpose is to illustrate the general behavior. At the moment of computing E/N, the ground-state energy per particle, we shall present the results for $U(S = 0)$. For completeness we have also computed E/N employing $U(S = 1)$ and the results were essentially unchanged. If on the other hand the two-body potential $V(r)$ should depend upon S, as it does in the nuclear case, the dependence $U(S)$ would then be very important.

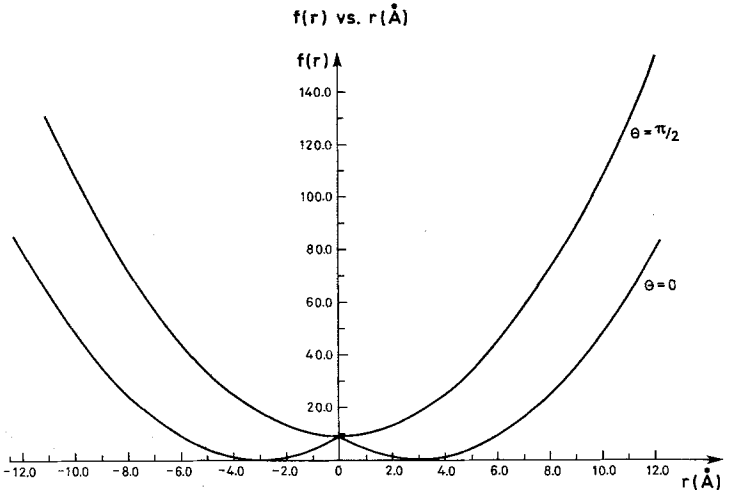

Fig. 1. The function $f(r)$ of Eq. (18) vs. r with $\Delta = 3$ Å, $\alpha^2 = 1.5$ Å^{-2} for two values of θ, the angle between **r** and **Δ**.

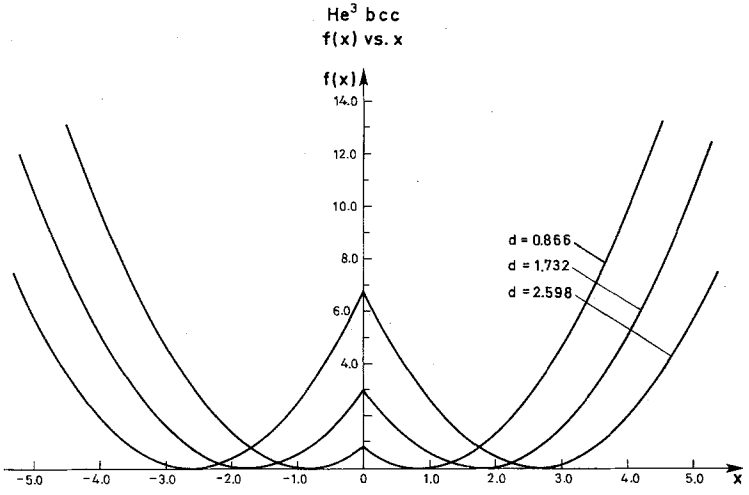

Fig. 2. $f(x)$ vs. $x = r/r_0$ for the first, fifth, and tenth shells of a bcc structure at $\theta = 0$. $d \equiv \Delta/r_0$, $r_0 = 4.3$ Å.

3. PARTIAL WAVE EXPANSION

We have used Eq. (17) for $U_s^{\pm}(\mathbf{r})$ in Eq. (3) to compute the ground-state energy for solid ^{3}He, using the *t*-matrix approach described in I. Since we are neglecting exchange effects and spin configuration we can use either

$U_s^+(\mathbf{r})$ or $U_s^-(\mathbf{r})$. For convenience, we have chosen $U_s^+(\mathbf{r})$. (U_s^- was tested in a few cases and gave almost identical results as U_s^+.) Upon making a partial wave expansion of $\psi(\mathbf{r})$

$$\psi(\mathbf{r}) = \sum_{l,\,\text{even}} (2l + 1)\psi_l(r)P_l(\mu) \tag{19}$$

the INGZ equation results in a set of coupled eigenvalue equations with eigenvalue η (l is even)

$$G_l''(x) + (\eta - E_l)G_l + \tfrac{1}{2}a^4 x d \sum_{l',\,\text{even}} (2l' + 1)W_{ll'}(x)G_{l'}(x) = 0 \tag{20}$$

where

$$W_{ll'}(x) = \int_0^1 \mu P_l(\mu)P_{l'}(\mu) \tanh\left(\tfrac{1}{2}\alpha^2 x\, d\mu\right) d\mu$$

In the above, the notation is as follows:

$$x = r/r_0, \qquad d = \Delta/r_0$$

$$\rho = m\gamma r_0^{-3} \qquad (\gamma = 4 \quad \text{fcc}; \quad \gamma = 2 \quad \text{bcc})$$

where ρ is the matter density, $a = \alpha r_0$, and moreover

$$G_l(x) = x\psi_l, \qquad \mu = \mathbf{r}\cdot\Delta/r\Delta$$

$$E_l = \frac{l(l+1)}{x^2} + \frac{1}{4}a^4x^2 + \frac{mr_0^2}{\hbar^2}V(x)$$

$$\eta = \frac{mr_0^2}{\hbar^2}E_{12} - \frac{2mr_0^2}{\hbar^2}U(0) - \frac{3}{2}a^2 - \frac{1}{4}a^4d^2$$

In the case of a neutron crystal, where the potential $V(\mathbf{r})$ depends on the spin configuration in the various states, a more general expansion for $\psi(\mathbf{r})$ that includes the spin wave function is necessary.

The energy per atom of the solid in the t-matrix approach is given by

$$E/N = \tfrac{3}{4}\hbar\omega + \tfrac{1}{2}\sum_k N_k\varepsilon_k \tag{21}$$

The first term is the kinetic energy per atom for a simple-harmonic-oscillator (SHO) potential, N_k is the number of particles in the kth shell, and ε_k is the shell energy given by

$$\varepsilon_k = \frac{\displaystyle\int_0^\infty \sum_l i^l(2l+1)j_l(Z_k)G_l(x)V(x)\{\exp[-\tfrac{1}{4}a^2(x^2 + d_k^2)]\}x\,dx}{\displaystyle\int_0^\infty \sum_l i^l(2l+1)j_l(Z_k)G_l(x)\{\exp[-\tfrac{1}{4}a^2(x^2 + d_k^2)]\}x\,dx} \tag{22}$$

where $Z_k \equiv ia^2 x d_k/2$, and $\Delta_k = r_0 d_k$; Δ_k is the distance from the atom under consideration to the kth shell and $j_l(Z)$ is the spherical Bessel function of order l. A bcc structure is assumed throughout.

The computation from now on is identical to that discussed in I, with the self-consistent requirement [cf. Eq. (30) in I]

$$U(0) \equiv \sum_k U_k = \sum_k N_k \varepsilon_k - \tfrac{3}{4}\hbar\omega \tag{23}$$

where U_k is now given by

$$U_k = 2\sqrt{2}\frac{N_k \int_0^\infty \sum_l i^l(2l+1) j_l(Z_k) G_l(x) V(x) \{\exp[-\tfrac{3}{4}a^2(x^2 + d_k^2)]\} x\, dx}{\int_0^\infty \sum_l i^l(2l+1) j_l(Z_k) G_l(x) \{\exp[-\tfrac{1}{4}a^2(x^2 + d_k^2)]\} x\, dx} \tag{24}$$

4. RESULTS AND DISCUSSIONS

The ground-state energy per atom for solid ^{3}He was determined using two different two-body potentials:

(a) The Lennard-Jones potential given by[1]

$$V(r) = 40.8[(2.556/r)^{12} - (2.556/r)^6]$$

(b) The Beck potential given by[1]

$$V(r) = V_0\left\{A[\exp(-\alpha r - \beta r^6)] - \frac{D}{(r^2 + p^2)^3}\left(1 + \frac{2.709 + 3p^2}{r^2 + p^2}\right)\right\}$$

TABLE I

Contributions per Particle to the Potential Energy for Solid ^{3}He (bcc) from the First Ten Shells Using the Lennard-Jones Potential at $\Omega = 21.0\,\text{cm}^3/\text{mole}$, $\alpha^2 = 1.68\,\text{Å}^{-2}$ [a]

Shell no. k	No. of particles N_k	Δ_k, Å	Shell energy ε_k, K	$\frac{1}{2}N_k\varepsilon_k$, K	U_k, K
1	8	3.564	−2.065	−8.261	−35.26
2	6	4.116	−2.262	−6.786	−16.66
3	12	5.820	−0.390	−2.342	−4.027
4	24	6.824	−0.136	−1.631	−2.809
5	8	7.129	−0.102	−0.407	−0.700
6	6	8.232	−0.040	−0.120	−0.203
7	24	8.969	−0.023	−0.2781	−0.4633
8	24	9.203	−0.020	−0.2366	−0.3916
9	24	10.080	−0.011	−0.1348	−0.2177
10	32	10.693	−0.008	−0.1251	−0.1988

[a] Kinetic energy = 20.38 K, potential energy = −20.32 K, E/N = 0.06 K.

TABLE II

Contributions per Particle to the Potential Energy for Solid ^{3}He (bcc) from the First Ten Shells Using the Lennard-Jones Potential at $\Omega = 23.0\ \text{cm}^3/\text{mole}$, $\alpha^2 = 1.44\ \text{Å}^{-2}$ [a]

Shell no. k	No. of particles N_k	Δ_k, Å	Shell energy ε_k, K	$\frac{1}{2}N_k\varepsilon_k$, K	U_k, K
1	8	3.672	−1.914	−7.656	−31.41
2	6	4.242	−1.981	−5.942	−14.47
3	12	5.998	−0.339	−2.032	−3.467
4	24	7.033	−0.117	−1.406	−2.421
5	8	7.347	−0.088	−0.350	−0.603
6	6	8.484	−0.034	−0.102	−0.174
7	24	9.243	−0.020	−0.236	−0.397
8	24	9.485	−0.017	−0.200	−0.335
9	24	10.389	−0.009	−0.113	−0.185
10	32	11.021	−0.007	−0.105	−0.169

[a]Kinetic energy = 17.43 K, potential energy = −18.14 K, E/N = −0.75 K.

where

$$V_0 = 10.371, \qquad A = 44.62 \times 10^4, \qquad \alpha = 4.39$$

$$D = 972.5, \qquad \beta = 3.746 \times 10^{-4}, \qquad p = 0.675$$

The above potentials are in K, with r measured in Å. The results are summarized in Tables I–V. We found that ten shells were sufficient to produce convergence to within ~0.5% in the sum over shells. In Fig. 3 we show the results of our E/N vs. molar volume Ω using the Lennard-Jones potential. (The result for the Beck potential coincides almost exactly with the Lennard-

TABLE III

Contributions per Particle to the Potential Energy for Solid ^{3}He (bcc) from the First Ten Shells Using the Lennard-Jones Potential at $\Omega = 23.94\ \text{cm}^3/\text{mole}$, $\alpha^2 = 1.35\ \text{Å}^{-2}$ [a]

Shell no. k	No. of particles N_k	Δ_k, Å	Shell energy ε_k, K	$\frac{1}{2}N_k\varepsilon_k$, K	U_k, K
1	8	3.724	−1.846	−7.384	−29.82
2	6	4.300	−1.869	−5.607	−13.60
3	12	6.080	−0.3181	−1.909	−3.242
4	24	7.129	−0.1097	−1.317	−2.266
5	8	7.448	−0.0820	−0.3279	−0.5645
6	6	8.600	−0.0317	−0.0951	−0.1627
7	24	9.370	−0.0183	−0.2190	−0.3708
8	24	9.615	−0.0155	−0.1857	−0.3126
9	24	10.531	−0.0088	−0.1051	−0.1728
10	32	11.171	−0.0061	−0.0973	−0.1575

[a]Kinetic energy = 16.32 K, potential energy = −17.25 K, E/N = −0.93 K.

TABLE IV

Contributions per Particle to the Potential Energy for Solid ^{3}He (bcc) from the First Ten Shells Using the Beck Potential at $\Omega = 21.0\ \text{cm}^3/\text{mole}$, $\alpha^2 = 1.81\ \text{Å}^{-2}$ [a]

Shell no. k	No. of particles N_k	Δ_k, Å	Shell energy ε_k, K	$\frac{1}{2}N_k\varepsilon_k$, K	U_k, K
1	8	3.564	−2.305	−9.211	−38.74
2	6	4.116	−2.480	−7.439	−18.05
3	12	5.820	−0.376	−2.258	−3.823
4	24	6.824	−0.126	−1.512	−2.585
5	8	7.129	−0.0938	−0.375	−0.641
6	6	8.232	−0.036	−0.109	−0.183
7	24	8.969	−0.021	−0.253	−0.417
8	24	9.203	−0.0179	−0.215	−0.352
9	24	10.080	−0.0102	−0.122	−0.195
10	32	10.693	−0.020	−0.319	−0.413

[a] Kinetic energy = 21.93 K, potential energy = −21.82 K, $E/N = 0.10$ K.

Jones curve.) Also shown are the experimental results.[5] The present results show better agreement with experiment over the previous ones, especially with regards to the slope of the curve.

The "wound integral"[1] κ was computed at $\Omega = 23.94\ \text{cm}^3/\text{mole}$, using the Lennard-Jones potential, and a value of 0.15 ($\ll 1$) was obtained. This indicates that the two-body approximation should be valid in this problem. Values of α^2 vs. Ω obtained in the present work are shown in Fig. 4 together with those of I and recent results of Pandharipande[6] and Domany *et al.*[7]

TABLE V

Contributions per Particle to the Potential Energy for Solid ^{3}He (bcc) from the First Ten Shells Using the Beck Potential at $\Omega = 23.0\ \text{cm}^3/\text{mole}$, $\alpha^2 = 1.53\ \text{Å}^{-2}$ [a]

Shell no. k	No. of particles N_k	Δ_k, Å	Shell energy ε_k, K	$\frac{1}{2}N_k\varepsilon_k$, K	U_k, K
1	8	3.672	−2.108	−8.430	−34.34
2	6	4.242	−2.149	−6.448	−15.59
3	12	5.998	−0.327	−1.962	−3.294
4	24	7.033	−0.109	−1.306	−2.232
5	8	7.347	−0.0808	−0.323	−0.5532
6	6	8.484	−0.0310	−0.0929	−0.1576
7	24	9.243	−0.0178	−0.2139	−0.3573
8	24	9.485	−0.01512	−0.1814	−0.3013
9	24	10.389	−0.0086	−0.1026	−0.1664
10	32	11.021	−0.0059	−0.0949	−0.1515

[a] Kinetic energy = 18.47 K, potential energy = −19.15 K, $E/N = -0.68$ K.

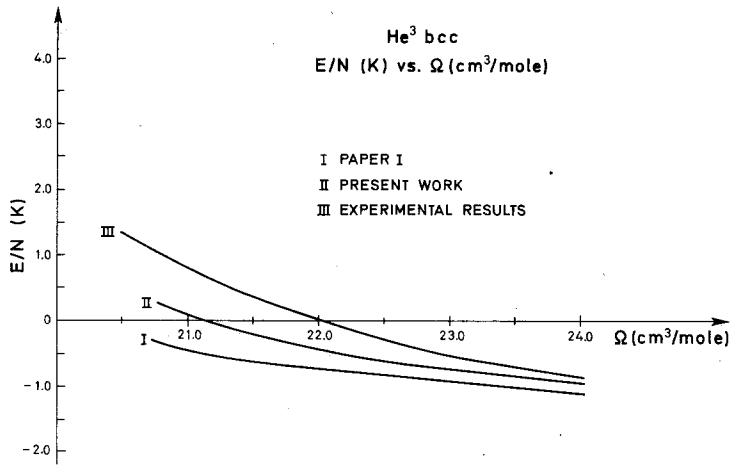

Fig. 3. E/N (K) vs. Ω (cm^3/mole) of the present work and paper I, both using the Lennard-Jones potential, compared with the experimental results.

We also computed the average correlation function $\bar{g}$ for the first and fourth shells using the Lennard-Jones potential at $\Omega = 23.94$ cm^3/mole. The results are qualitatively the same as in I and are shown in Fig. 5.

The close agreement between the results of the present calculation and experiment for the ground-state energies of solid ^{3}He, a quantum solid,

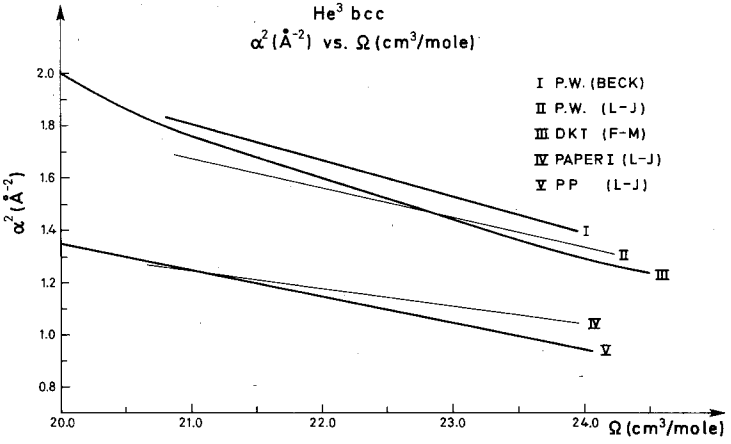

Fig. 4. α^2 (Å^{-2}) vs. Ω (cm^3/mole) obtained in the present work (P.W.) with Beck and Lennard-Jones potentials compared with those of paper I, Pandharipande (PP), who used the Lennard-Jones potential, and of Domany, Kirson, and Thieberger (DKT), whose used the Frost–Musulin potential (FM).

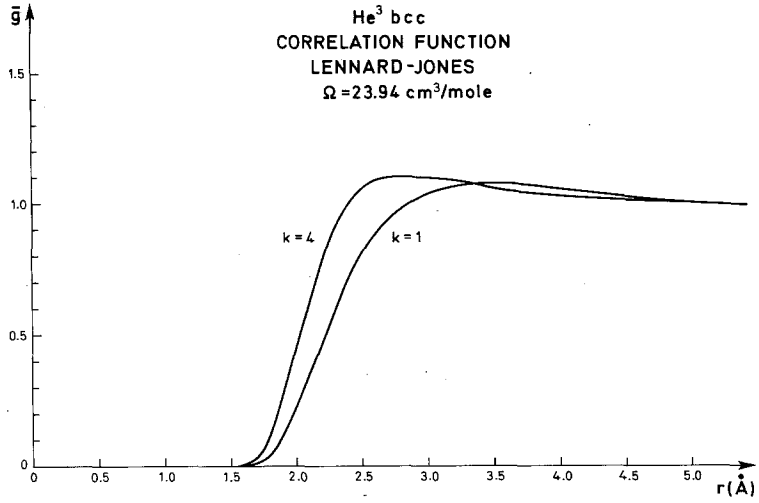

Fig. 5. Average correlation function $\bar{g}$ for the first and fourth shells using the Lennard-Jones potential at $\Omega = 23.94\,\text{cm}^3/\text{mole}$.

indicates that this method should be applicable to other quantum solids as well, in particular, solid neutrons. However, the neutron solid problem is more complex because of the complicated dependence of the two-body potential on spin and angular momentum. Furthermore, there are no nucleon–nucleon two-body potentials that are as reliable as those for solid ^{3}He. Preliminary results on neutron solid computations using the symmetric $U_s(r)$ do indicate substantial differences between Reid[8] and Bethe–Johnson[9] two-body potentials, even though they both reproduce nucleon–nucleon scattering phase shifts equally well.

5. CONCLUSION

The symmetric one-body potential described in Section 2 has several interesting features. First of all, it improves considerably the single-particle energies with respect to the results of I, as indicated in Fig. 3. Not only is the curve of E/N closer to the experimental curve, but the slope is also improved, thus producing better values of the sound velocities and elastic constants.

The general shape of $U_s(r)$ is also of importance for the study of nuclear fission where a double-well, one-body potential of that shape is needed. The only clipped harmonic oscillator so far published[10] has an unphysical spike at $r = 0$, thus making the determination of the eigenvalues through a matching condition a cumbersome problem.

Finally, Eq. (17) solves one of the problems encountered in the description of a possible quantum solid of neutrons at densities encountered in the deep interior of most neutron stars. A parity-violating Hamiltonian such as the one used in II and in all the subsequent work on the same subject by other authors brings into the game waves like $^3S_1$ that the Pauli principle would not allow. The present form of $U_s(r)$ allows only the properly symmetrized wave function $\psi(\mathbf{r})$ to contribute and therefore only the permissible nuclear matrix elements. The neutron quantum solid computation is now being repeated and the results will be published elsewhere.

ACKNOWLEDGMENT

Two of the authors (V.C. and J.L.) would like to express their thanks to Prof. B. Strömgren and Prof. A. Bohr for their hospitality at NORDITA—Niels Bohr Institute.

REFERENCES

1. V. Canuto, J. Lodenquai, and S. M. Chitre, *Phys. Rev. A* **8**, 949 (1973).
2. V. Canuto, J. Lodenquai, and S. M. Chitre, *Solid State Commun.* **13**, 709 (1973).
3. V. Canuto and S. M. Chitre, *Phys. Rev. Letters* **30**, 999 (1973).
4. B. Bradow, *Ann. Phys. (N.Y.)* **74**, 112 (1972), Sec. VII.
5. R. C. Pandorf and D. O. Edwards, *Phys. Rev.* **169**, 222 (1968).
6. V. R. Pandharipande, private communication.
7. E. Domany, M. W. Kirson, and R. Thieberger, *Phys. Rev. A* **8** 4, 1937 (1973).
8. R. V. Reid, *Ann. Phys. (N.Y.)* **50**, 411 (1968).
9. M. Johnson, private communication.
10. P. Holzer, U. Mosel, and W. Greiner, *Nucl. Phys.* **A138**, 241 (1969).